



# Synthesis and characterization of hybrid activated bentonite/alginate composite to improve its effective elimination of dyes stuff from wastewater

Amina Aichour<sup>1</sup> · Hassina Zaghouane-Boudiaf<sup>1</sup>

Received: 4 October 2018 / Accepted: 13 May 2020 / Published online: 24 May 2020  
© The Author(s) 2020

## Abstract

The current paper is paying attention to the synthesis of a low-cost, abundant and efficient hybrid activated bentonite–alginate composite ABent/A. Hybrid composite morphology was determined through FTIR, XRPD, and  $\text{pH}_{\text{PZC}}$ . The operational conditions for the retention of two dyes used in the textile industry (methylene blue and crystal violet) from aqueous mediums were evaluated. Results showed that MB and CV adsorbed amount on ABent/A was 780 and 546 mg/g, respectively. Kinetic Lagergren's and Ho and McKay's models provide the best result for the MB and CV adsorption on the prepared adsorbent, respectively. Langmuir isotherm model gives the best analyses of the experimentation, justifying a monolayer and a homogeneous nature of adsorption process. Results indicate also that the operational conditions studied affect significantly dyes removal. Reusability study of ABent/A for dyes was also investigated according to the type of desorbing agents. MB regeneration was found 98.92% using hydrochloric acid 0.01 M and CV regeneration percent was 95% using 0.5 M potassium chloride prepared in the mixture ethanol/water (0.5%/0.5%). From the obtained results, hybrid activated bentonite/alginate composites are low-cost, effective and regenerable adsorbent, which give a promising prospect for contaminated wastewaters treatment.

**Keywords** Adsorption · Activated bentonite · Alginate · Composite · Cationic dyes · Regeneration

## Introduction

Most industries have used colors in their products (Bertolini et al. 2013; Jauris et al. 2016). It is known that the concentration of cationic dyes during the process of coloration of products is very high, and it was estimated that from 5 to 15% of these dyes was lost and discharged in wastewaters which cause many health and environmental issues (Dellamatrice et al. 2017). Methylene blue (MB) exists in several hydrated forms (Rager et al. 2012). It is commonly applied as an organic model of contaminant because of its stable molecular structure (Fu et al. 2015). The toxicological data

relating to the use of the methylene blue at humans have indicated the absence of danger related to the use of this product like the drug (Rafatullah et al. 2010). Recently, it was observed that it can cause thoracic pains, a dyspnea; an anxiety, tremors, hypertension, and even a coloring of the skin if the amount is high. Crystal violet (CV) is a carcinogenic dye that declared as insubordinate molecules. It can be absorbed causing irritation and is harmful by inhalation and ingestion. Its most harmful effects are blindness and cancer (Mittal et al. 2010).

Many water treatment methods were successfully applied in the elimination of different kinds of contaminants, especially dyes, such as adsorption (Wang et al. 2013; Guz et al. 2014), photocatalysis (Peng et al. 2016; Sandoval et al. 2016; Li et al. 2016), coagulation–flocculation (Papic et al. 2000, 2004), and combined process such as coagulation–adsorption (Kuppusamy et al. 2017).

Recently, adsorption process is considered a competitive, efficient and promising technique to be used in the elimination of contaminants. It seems to offer the best prospects for displacement of pollutants from the aqueous medium.

✉ Amina Aichour  
aichouramina2@gmail.com  
Hassina Zaghouane-Boudiaf  
boudiafhassina2000@yahoo.fr

<sup>1</sup> Chemical Engineering Process Laboratory (LCEP),  
Chemical Engineering Department, Faculty of Technology,  
University of Ferhat Abbas Setif-1, 19000 Sétif, Algeria

Actually, emphasis has been placed on the preparation of inexpensive, non-polluting active substances to be used in the cleanup of polluted water.

According to the beneficial properties of clays such as the availability, ecologically friendly, not polluted, they make its use become more focused by researchers (Boualla and Benziane 2011; Zaghouane-Boudiaf and Boutahala 2011; Auta and Hameed 2014; Anirudhan and Ramachandran 2015; Hassani et al. 2015; Derafa et al. 2018).

Certain problems arise nevertheless in their implementation with a difficulty of separation of treated water and especially of their regeneration. The encapsulation with biopolymers makes it possible to mitigate this problem (Lezehari et al. 2010; Tezcan et al. 2012; Pandi and Viswanathan 2014; Tan and Ting 2014; Jung et al. 2016).

The alginate is a polymer of the family of polysaccharides, most used for this intent. Alginate has many properties suitable for adsorption process, among them, gelation property which is considered the very important property because it has the ability for combining different matters together through egg-box structure assured by the interaction between the divalent metals, the process named encapsulation (Ely et al. 2011). So, the realization of adsorbent composite beads can be implemented in processes of water treatment not only in discontinuous but especially continuous processes (Cheng et al. 2012; Abdollahi et al. 2013; Kumar et al. 2013).

This work investigates a suitable and very interesting method to synthesize hybrid activated bentonite/alginate composite beads as efficient adsorbent; the characterization of the adsorbent using FTIR, XRPD, and  $\text{pH}_{\text{PZC}}$  analysis. The investigation of adsorption process for the cleanup of water from dyestuff, methylene blue (MB) and crystal violet (CV) were chosen as pollutant models due to their wide applicability in the industries, and their toxicity, using the obtained adsorbent. Finally, the reuse of the composite several times was studied to economize the process.

## Experimental section

### Materials

Natural clay used in this research was provided from Maghnia deposit (Algeria) type bentonite. Methylene blue ( $\text{C}_{16}\text{H}_{18}\text{N}_3\text{S}\text{Cl}$ ) abbreviated as MB and crystal violet ( $\text{C}_{25}\text{H}_{30}\text{N}_3\text{Cl}$ ) abbreviated as CV were provided by Appli-Chem Panreac ITW Companies. Sulfuric acid, sodium alginate and calcium chloride were provided from Sigma-Aldrich and R&M Chemicals, respectively.

### Synthesis of activated bentonite/alginate composites

The preparation of activated bentonite was done by the same procedure used previously by Zaghouane-Boudiaf et al. (2014); sample was named (ABent).

Activated bentonite/alginate hybrid beads (ABent/A) were prepared by extrusion method, using 2 g alginate was dissolved in 100 mL of distilled water, then an equal mass of ABent was added (2/2; alginate/ABent; m/m). The extrusion method consists of introducing of alginate solution or alginate containing the encapsulated material drop by drop using a syringe or a pipette tip through a peristaltic pump into a solution containing the crosslinker ( $\text{CaCl}_2$  4%). Fast reaction between sodium alginate and reticulated agent ( $\text{CaCl}_2$ ) makes it possible to solidify the spherical shape of the drop within the solution. This method leads to the depiction of millimetric-diameter size. Mixture of beads and calcium chloride was left at magnetic agitation for one night to insure the maturation of beads. Beads were cleaned using deionized water until pH of water became 7, and then dried at room temperature.

### Instrumental characterization

FTIR analysis of the samples was carried out in KBr pellets in the interval of  $400\text{--}4000\text{ cm}^{-1}$  using FTIR 8400S apparatus type Shimadzu having a standard mid-IR DTGS detector.

X-ray powder diffraction was done using a Philips® X-Pert diffractometer, equipped with automatic crack,  $\text{CuK}\alpha$  radiation, and a graphite monochromator.

The determination of the point of zero charge of samples was done using 1/1 mass/volume ratio, the initial pH solution of deionized water was adjusted using 0.01 M hydrochloric and sodium hydroxide solutions to prepare acidic and basic mediums, samples were added under stirring for 48 h at  $24\text{ }^\circ\text{C}$ . Final pH was measured.

### Experimentation of dyes removal

Adsorption isotherms of dyes were investigated in different feed concentrations 25–2200 mg/L, other operational conditions were maintained constants such as  $T=24\text{ }^\circ\text{C}$ ,  $\text{pH}_{\text{MB}}=6.4$ ,  $\text{pH}_{\text{CV}}=5.9$ . The adsorption capacity of dyes at equilibrium, and the removal were accounted using Eqs. (1) and (2) below:

$$q_e = \frac{(C_0 - C_e)V}{m} \quad (1)$$

$$R(\%) = \frac{C_0 - C_e}{C_0} * 100 \quad (2)$$

where  $q_e$  (mg/g),  $R$  (%),  $C_0$ ,  $C_e$  (mg/L),  $V$  (L) and  $m$  (g) are the removal capacity of dyes at the end of adsorption process; removal percent of dyes; the feed and the ataxy concentrations of dyes; the volume of feed dye solution; and the adsorbent mass, respectively.

The combination between the operational conditions, contact time and the initial concentration of dyes with adsorption process was studied in a range of concentration of 25–300 mg/L, at room temperature ( $T = 24 \text{ }^\circ\text{C} \pm 1 \text{ }^\circ\text{C}$ ) without pH adjustment ( $\text{pH}_{\text{MB}} = 6.4$ ,  $\text{pH}_{\text{CV}} = 5.9$ ). 100 mg of ABent/A was mixed with 100 mL of MB and CV solutions and shacked at 200 rpm. After each time of contact, a sample of dye was removed and analyzed at 664 and 590 nm.

Adsorption capacity relationship is given by Eq. (3):

$$q_t = \frac{(C_0 - C_t)V}{m} \quad (3)$$

where  $C_0$ ,  $C_t$  (mg/L);  $V$  (L); and  $m$  (g) are the feed and the residual concentrations of dyes; the volume of feed dye solution; and the adsorbent mass, respectively.

The impact of pH was investigated in MB and CV pH interval of 2–11 and 3–11, respectively, by adjustment of feed dyes solutions of 100 mg/L using 0.1 M of HCl and NaOH solutions. 10 mg of ABent/A was added to 10 mL of dyes solution and shaken at 200 rpm and at temperature of  $24 \pm 1 \text{ }^\circ\text{C}$ .

Temperature influence on the equilibrium adsorption was studied at 10, 20, 30 and 40  $^\circ\text{C}$ , at natural pH of dyes solution ( $\text{pH}_{\text{MB}} = 6.4$ ,  $\text{pH}_{\text{CV}} = 5.9$ ). Initial concentration of methylene blue and crystal violet was 100 mg/L, the adsorbent mass was 10 mg and the volume of MB and CV solution was 10 mL.

## Experimental modeling

### Isotherms modeling

The modeling of the experimental data of the isotherms is for aim to know the adsorption capacity of ABent/A, also to evaluate the mechanisms applied in the adsorption process. The well-known isotherm models; Langmuir, Freundlich, Dubinin–Radushkevich and Toth were applied to fit the experimental data.

#### 1. Langmuir isotherm (Langmuir 1918)

Langmuir model justifies a monolayer and homogeneous adsorption

$$q_e = \frac{q_m K_L C_e}{1 + K_L C_e} \quad (4)$$

where  $q_m$  (mg/g);  $K_L$  are the Langmuir maximum adsorption capacity of the ABent/A; and Langmuir's constant.

#### 2. Freundlich isotherm (Freundlich 1906)

Freundlich propose that the adsorption is made on multi-layer and heterogeneous in nature

$$q_e = K_F C_e^{1/n} \quad (5)$$

where  $K_F$  and  $n$  are the Freundlich adsorption coefficient and the exponential coefficient.

#### 3. Dubinin–Radushkevich isotherm (Dubinin and Radushkevich 1947)

This model was chosen to assess the energy of the process and the porosity of the adsorbent.

$$q_e = q_s \cdot e^{-B \cdot \varepsilon^2} \quad (6)$$

$$\varepsilon = R \cdot T \cdot \ln \left( 1 + \frac{1}{C_e} \right) \quad (7)$$

where  $q_s$  (mg/g),  $B$  ( $\text{mol}^2/\text{kJ}^2$ ) and  $\varepsilon$  are equilibrium removal capacity, constant of the  $D$ – $R$  model, and the Polanyi potential.

From the constant  $B$ , the adsorption energy  $E$  (kJ/mol) could be evaluated using the equation below:

$$E = \frac{1}{\sqrt{2 \cdot B}} \quad (8)$$

#### 4. Toth isotherm (Toth 1962)

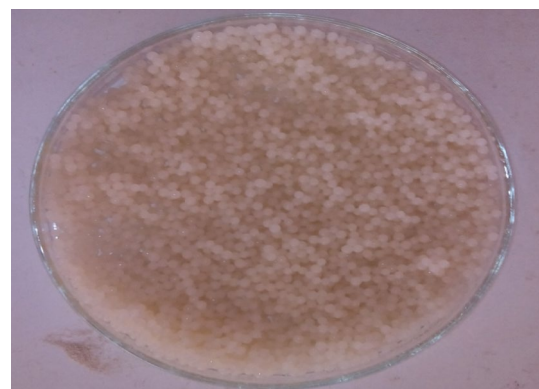
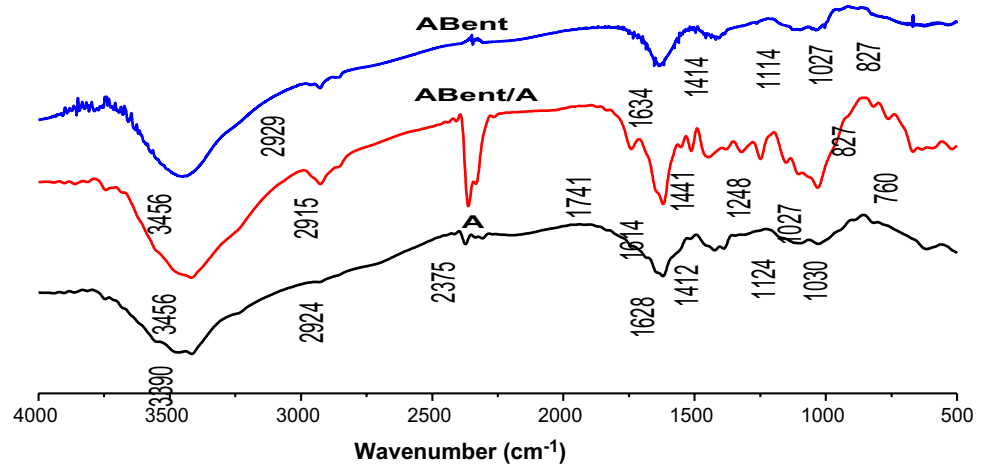
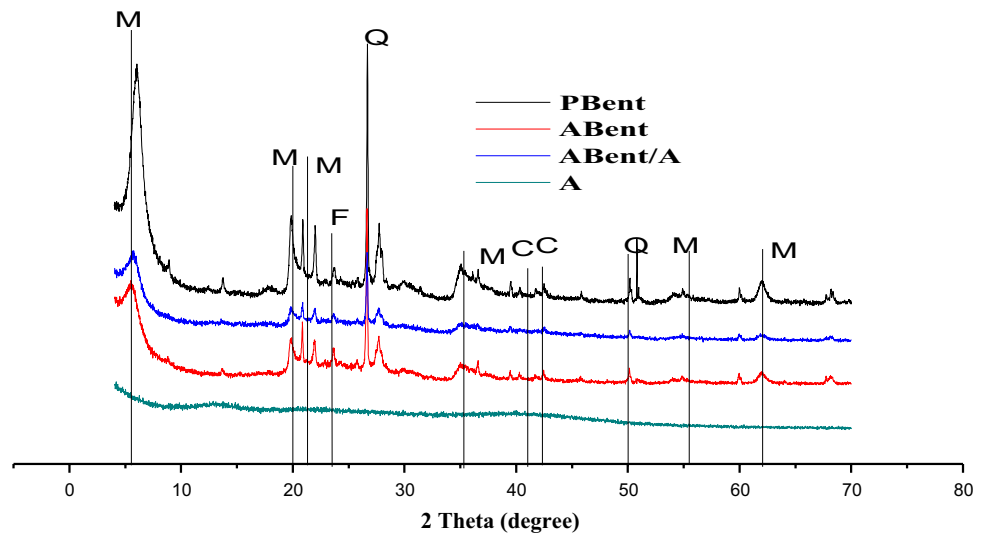


Fig. 1 Activated bentonite/alginate (ABent/A) wet beads

**Fig. 2** FTIR spectrum of ABent, A and ABent/A



**Fig. 3** XRD specters of the PBent, ABent, ABent/A, and alginate (A)



The model was chosen to minimize the error of found by Langmuir model. It is a special type from Langmuir isotherm similar to BET isotherm.

$$q_e = \frac{q_{\max T} \cdot C_e}{\left(\frac{1}{K_T} + C_e^{m_T}\right)^{1/m_T}} \quad (9)$$

where  $q_e$  (mg/g);  $q_{\max T}$  (mg/g);  $C_e$  (mg/L);  $K_T$  and  $m_T$  are the maximum adsorption capacity at equilibrium found experimentally; the maximum adsorption capacity of Toth model; the equilibrium concentration, and Toth's parameters.

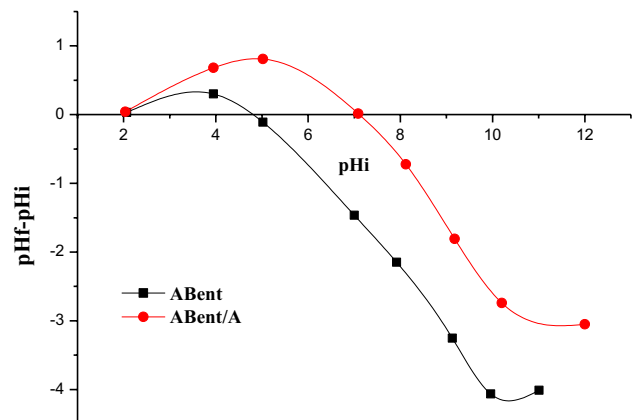


**Fig. 4** Zero charge points of ABent and ABent/A

### Kinetics modeling

To understand kinetics and to quantify adsorption changes over time, two models are used:

- (1) The pseudo-first-order kinetic model proposed by Lagergren (1898): for solid/liquid adsorption process.

$$q_t = q_e(1 - \exp^{-k_1 t}) \tag{10}$$

where  $q_e$ ,  $q_t$ , and  $k_1$  are the dye adsorption capacities at final of the experiment and at any time  $t$  (min); and the constant of Lagergren kinetic model, respectively.

- (2) The pseudo-second-order kinetic model proposed by Ho and McKay (1999):

$$q_t = \frac{q_e^2 k_2 t}{1 + q_e k_2 t} \tag{11}$$

where  $k_2$  (g/mg min) is the constant of Ho and McKay kinetic model.

### Error analysis

So as to assess the relevance of kinetic and isotherm models, correlation coefficient ( $R^2$ ) and the residual root-mean-square error (RMSE) have been used. They are given by the following expressions:

$$R^2 = \frac{1 - \sum_{n=1}^n (q_{e,exp,n} - q_{e,cal,n})^2}{\sum_{n=1}^n (q_{e,exp,n} - q_{e,cal,n})^2} \tag{12}$$

$$RMSE = \sqrt{\frac{1}{n-1} \sum_{n=1}^n (q_{e,exp} - q_{e,cal})^2} \tag{13}$$

### Reusability study

Reusability of adsorbents is considered as an economic factor which minimizes the cost of the adsorption process, to show the possibility of reusing ABent/A composite beads several times, MB and CV were regenerated using various desorbing agents. MB desorption was evaluated using hydrochloric acid solution in two different concentrations (0.1 M, 0.01 M), while CV desorption was studied using different solutions (0.5 M acetic acid solution, 100% ethanol solution, 0.5 M potassium chloride solutions and 0.5 M potassium chloride prepared in the mixture ethanol/water (0.5%/0.5%). Adsorption of dyes was done in the same way presented in the section of kinetics study. After adsorption, the saturated beads were washed and dried at 24 °C. 100 mL of each desorbing agent was added to ABent/A composites and shaken for equilibrium time (48 h). MB and CV samples were analyzed. MB and CV adsorption-desorption were repeated many times to assess the regeneration of the composites.

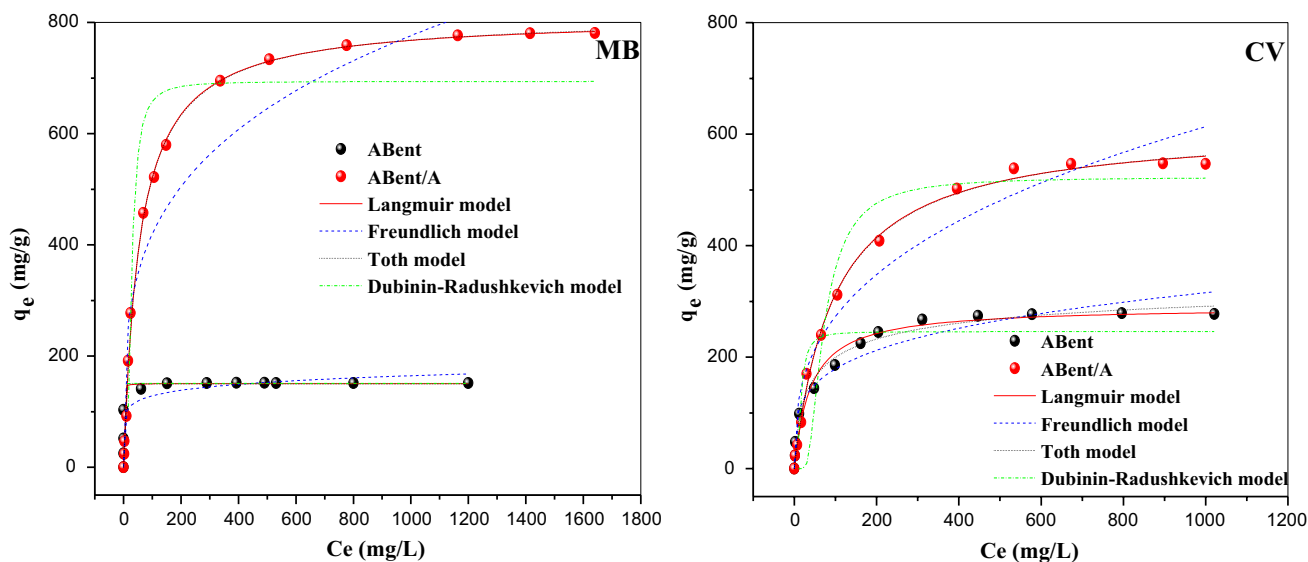


**Fig. 5** Isotherms of MB and CV adsorption onto ABent and ABent/A ( $C_0=25\text{--}2500$  mg/L,  $V=10$  mL,  $m=10$  mg,  $Agit=200$  rpm and  $T=25$  °C)

**Table 1** Parameters of isotherm models for the adsorption of MB and CV onto adsorbents

Models	Parameters	Methylene blue		Crystal violet	
		ABent	ABent/A	ABent	ABent/A
Langmuir	$q_e$ (mg/g)	150.71	810.27	290.37	614.38
	$K_L$ (L/mg)	2.808	0.018	0.025	0.010
	$R^2$	0.936	0.998	0.975	0.997
	RMSE	14.43	14.46	16.83	12.62
Freundlich	$K_F$ ((mg/g)(L/mg) <sup>1</sup> )	78.27	122.39	57.63	54.04
	$n$	0.108	0.267	0.246	0.352
	$R^2$	0.872	0.904	0.943	0.951
	RMSE	20.35	96.29	25.29	49.09
Dubinin–Radushkevich	$q_s$ (mg/g)	150.78	693.95	245.86	523.04
	$B$ (mol <sup>2</sup> /kJ <sup>2</sup> )	$5.62 \times 10^{-8}$	$8.81 \times 10^{-5}$	$2.87 \times 10^{-5}$	$6.20 \times 10^{-4}$
	$E$ (kJ/mol)	2982.75	75.34	28.40	111.66
	$R^2$	0.950	0.919	0.952	0.914
Toth	$q_e$ (mg/g)	150.15	813.09	358.74	618.66
	$K_T \times 10^3$	9840	0.05	0.314	0.012
	$m_T$	20.73	0.982	0.490	0.980
	$R^2$	0.952	0.998	0.987	0.996
	RMSE	12.39	15.01	12.06	13.22

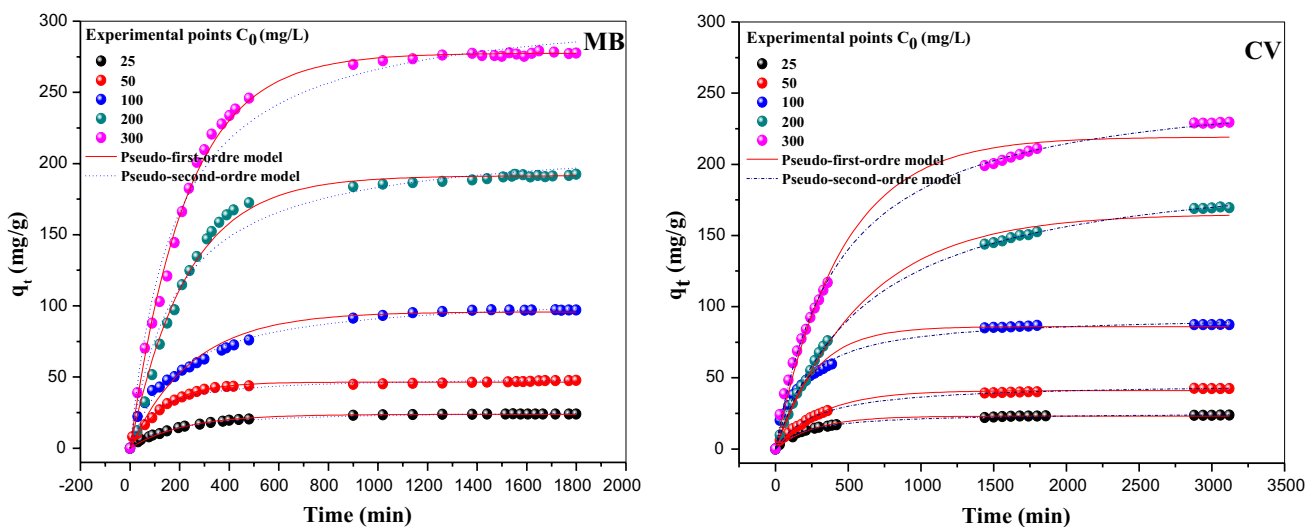


**Fig. 6** Experimental data and modeling of adsorption kinetics of MB and CV onto ABent/A beads ( $C_0=25\text{--}300$  mg/L,  $m=100$  mg,  $V=100$  mL, Agit=200 rpm,  $T=25$  °C,  $pH_{MB}=6.4$ ,  $pH_{CV}=5.9$ )

## Discussion of the results

### Characterization

The photo of ABent/A wet composites beads is shown in Fig. 1. The color with which the beads look indicates that bentonites are well-encapsulated.

The FTIR spectra of ABent, ABent/A beads and alginate referred as (A) shown in Fig. 2 gives similar bands. The

picks at  $3390\text{ cm}^{-1}$ , and  $3456\text{ cm}^{-1}$  and  $3420\text{ cm}^{-1}$  in the spectrum of alginate beads (A) and ABent/A are specified to the vibrations of OH (hydroxyl) groups. The bands at  $1590\text{--}1629\text{ cm}^{-1}$  and at  $1417\text{--}1420\text{ cm}^{-1}$  observed in the spectra of alginate (A) are assigned to C–O–O asymmetric and symmetric stretching of alginate molecule (Oladipo and Gazi 2014). The bands at  $2924\text{ cm}^{-1}$ ,  $1124\text{ cm}^{-1}$ , and at  $1030\text{ cm}^{-1}$  are referred to CH stretching vibration, CO stretching of ether groups and CO stretching of alcoholic

**Table 2** Kinetic parameters for MB and CV adsorption onto ABent/A

Dyes	Concentration (mg/L)	Pseudo-first-order					Pseudo-first-order				
		$Q_{e,exp}$	$Q_{e,cal}$	$K_1$	$R^2$	RMSE	$Q_{e,exp}$	$K_2$	$R^2$	RMSE	
MB	25	23.87	23.81	4.62	0.994	0.523	25.92	25.02	0.993	0.583	
	50	47.67	47.06	6.97	0.993	1.063	50.07	22.26	0.983	1.742	
	100	97.03	96.25	3.96	0.969	4.885	105.04	530.59	0.989	2.926	
	200	192.60	192.63	4.32	0.993	4.705	212.02	270.33	0.967	10.557	
	300	277.63	277.91	4.42	0.996	4.649	304.48	198.24	0.976	12.431	
CV	25	23.75	23.088	3.67	0.990	0.692	25.486	19.05	0.998	0.306	
	50	42.33	41.018	3.13	0.993	1.131	46.443	783.19	0.998	0.464	
	100	87.27	85.973	3.80	0.975	4.050	94.302	540.11	0.992	2.313	
	200	169.54	165.164	1.64	0.995	4.251	205.543	7695.13	0.999	1.104	
	300	229.55	219.222	2.23	0.989	8.117	260.599	8918.18	0.998	2.662	

$k_1$  (1/min).10<sup>3</sup>,  $k_2$  (g/mg min)10<sup>3</sup>,  $q_{e(exp, cal)}$  (mg/g)

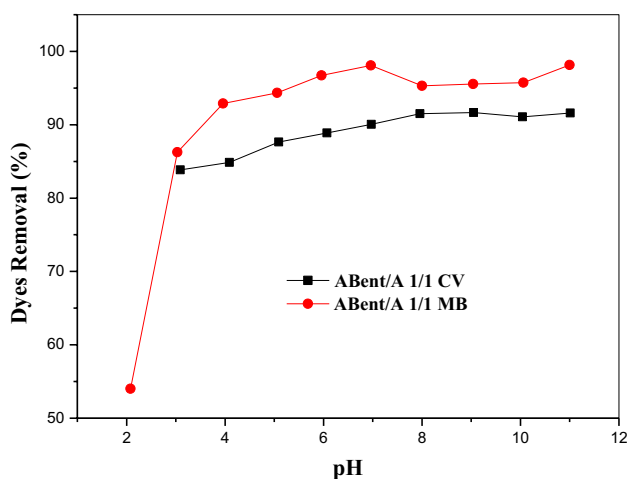


**Fig. 7** pH impact on the adsorption of dyes on ABent/A ( $C_0=100$  mg/L,  $m_{ABent/A}=10$  mg,  $V_{ABent/A}=10$  mL, Agit=200 rpm,  $T=25$  °C)

groups, respectively (Vijaya et al. 2008; AbouTaleb et al. 2012).

XRD patterns of Natural bentonite (Bent), ABent, ABent/A, and alginate are given in Fig. 3. The XRD pattern of purified bentonite (Bent) showed the  $d_{001}$  reflection at 2 theta = 5.686. The spacing correspondent to the inter-coat is 1.91 nm. Bentonite is characterized by four peaks, first is located at 15.037 Å and the three others are at 4.508 Å, 2.567 Å and 1.501 Å. This diffractogram shows that the minerals nonargillaceous present in variable quantities from one sample to another is mainly quartz with characteristic reflexions with  $d_{001}=3.35$  Å and 4.28 Å, calcite ( $d_{001}=3.21$  Å), and of the feldspars ( $d_{001}=4.06$  Å). XRD spectrum shows that acid treatment made some changes in the structure of the bentonite.

XRD analysis shows the crystallinity variation which is an important parameter whose evolution reflects a modification of

the microstructure when alginate introduced to bentonite. Figure 3 shows also a low in line of alginate pattern which indicate the amorphous structure. The value of  $d_{001}$  for the composite ABent/A stay equal to  $d_{001}$  of ABent which is a sign that alginate has not intercalated in the bentonite silicate film, interactions between the carboxylic group of alginate and the positive charge of the montmorillonite led to their link. The found results are confirmed by FTIR analysis founded previously (Chen et al. 2015).

The point of zero charges of adsorbents was shown in Fig. 4. They are 4.7 and 7.04, respectively for ABent and ABent/A. The point of zero charge results revealed that the surfaces are highly acidic and neutral, respectively, for ABent and ABent/A. So adsorbents are attractors of cations.

### Impact of the operational conditions on the elimination of dyes

#### Adsorption isotherms

In general, adsorption isotherms provide information on adsorption capacity; the optimization and the design of the adsorbents; they describe the affinity between adsorbate and adsorbent.

MB and CV adsorption isotherms onto ABent and ABent/A are represented in Fig. 5. Both of MB and CV adsorption isotherms had the same allure, they reveal when the feed concentration of MB and CV increase, the adsorbed quantity increases until a stage indicating the fullness of adsorbent; what shows that the MB and CV adsorbs in a homogeneous way assured by the negative ionic interactions found on the adsorbent surface. Adsorbed capacities of MB onto ABent and ABent/A were 151 and 780 mg/g, respectively. CV adsorption capacities onto ABent and ABent/A were 277 and 546 mg/g, respectively. The highest adsorbed amount of MB comparing with CV adsorbed amount is due to the size of the molecules, the size of CV molecule is bigger than MB molecule (Abbasi et al. 2017).

**Fig. 8**  $\ln(q_e/C_e)=f(1/T)$  plot for dyes adsorption onto ABent/A ( $C_0=100$  mg/L,  $m_{\text{ABent/A}}=10$  mg,  $V_{\text{ABent/A}}=10$  mL, Agit=200 rpm,  $\text{pH}_{\text{MB}}=6.4$ ,  $\text{pH}_{\text{CV}}=5.9$ )

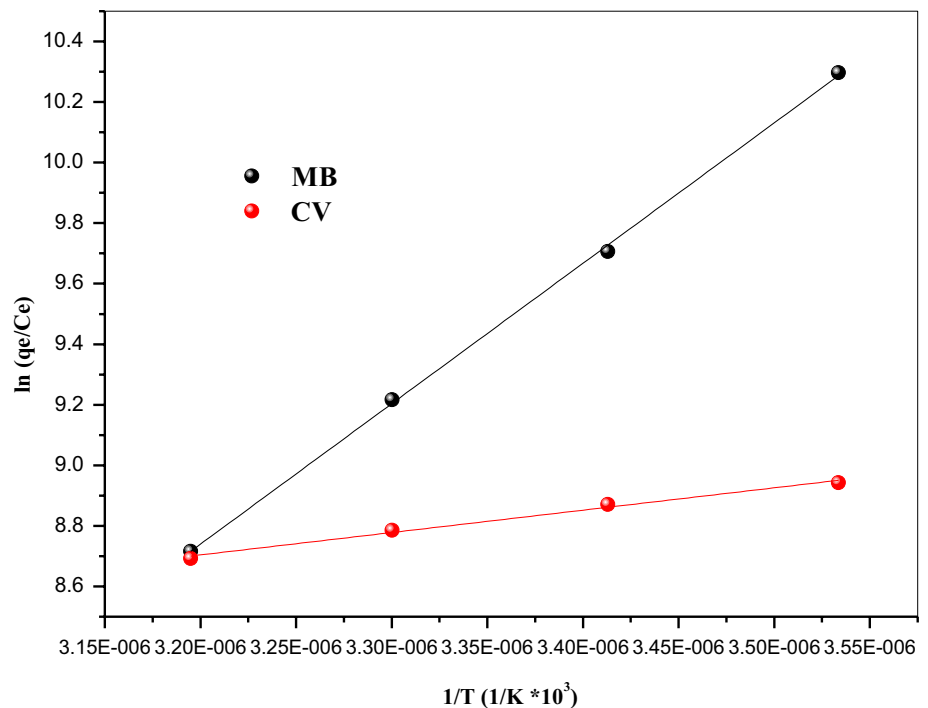


**Table 3** Thermodynamic data for the adsorption of MB and CV onto ABent/A

T (K)	$\Delta G^\circ$ (kJ/mol)	$\Delta H^\circ$ (kJ/mol)	$\Delta S^\circ$ (J/mol K)
<b>MB</b>			
283	-38,545.65	$-38.65 \times 10^3$	-50.72
293	-38,545.14		
303	-38,544.63		
313	-38,544.13		
<b>CV</b>			
283	-6152.92	$-61.38 \times 10^2$	52.71
293	-6153.44		
303	-6153.97		
313	-6154.50		

The experimental data of MB and CV adsorption isotherms were modeling using the nonlinear regression of Langmuir, Freundlich, Dubinin–Radushkevich and Toth using Eqs. (4, 5, 6 and 9), isotherms modeling results are listed Table 1. The higher  $R^2$ , the lowest RMSE and the close calculated adsorption capacities using this isotherm model in comparison with the experimental capacities suggest that Langmuir isotherm is the optimum model can characterize and describe the process of dyes adsorption.

#### Impact of stirring time and feed concentration

Adsorption rate is very important to show the design and to evaluate kinetics parameters. MB and CV kinetics on

prepared adsorbent ABent/A at different concentrations 25–300 mg/L was studied, results are shown on Fig. 6. Adsorption kinetics of MB and CV dyes on ABent/A take the same form characterized by a strong adsorption dice first minutes of contact, followed by a slow stage until reaching equilibrium. For MB, equilibrium was reached at 7 and 24 h in the lowest and the highest concentrations, respectively, while in case of CV, the equilibrium time was found to be about 24 to 48 h for the lowest and the highest concentrations, respectively (Huang et al. 2017).

Adsorption kinetics were speedy in the starting of the experiment (first time of the reaction), and this is due to the existence of more active sites at the beginning of adsorption than that of the sites remaining after a certain time (Elmoubaraki et al. 2017).

The adsorption kinetics modeling results given in Table 2; the elevated  $R^2$  and lowest RMSE reveal that the Lagergren's model is the very suitable model can describe adsorption process in case of MB and Ho and McKay's model is the best for CV adsorption process.

#### Impact of pH

pH change can affect the ionization level of the dyes, also impact the functional groups dissociation, it can affect the stage of the elimination of dyes (Nandi et al. 2009), the obtained result of pH impact on dyes elimination onto ABent/A are given in Fig. 7. MB and CV retention were very influenced by pH, the removal (%) was increasing with the rise up of pH until  $\text{pH}=8$  and remains steady at the



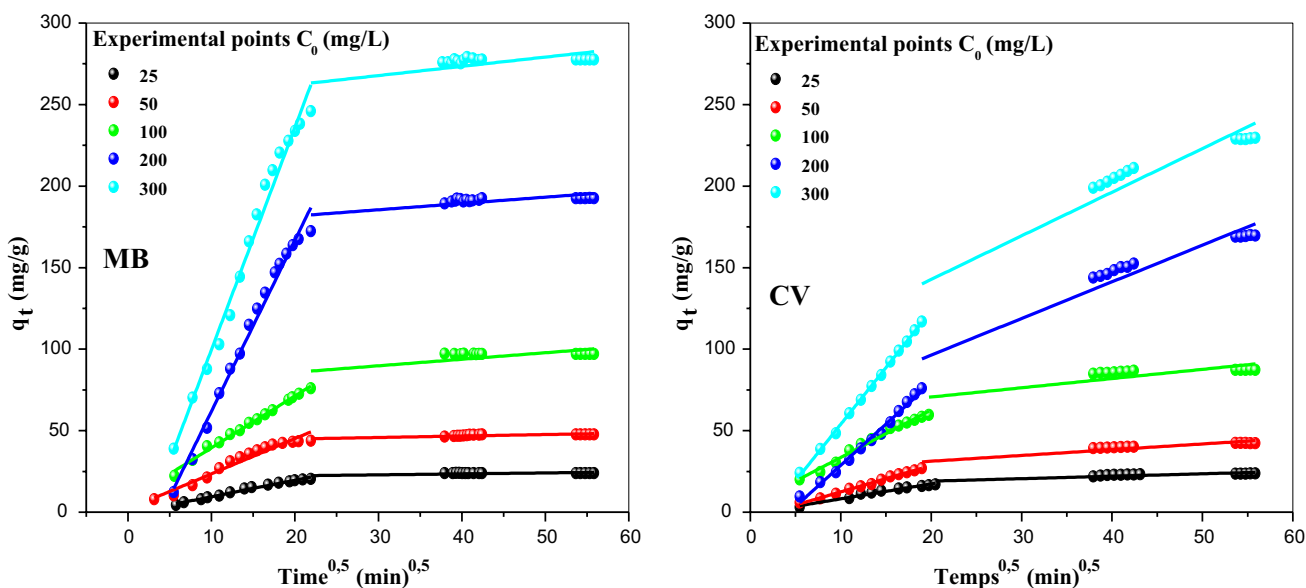


Fig. 9 Intraparticle diffusion model for dyes adsorption onto ABent/A

Table 4 Intraparticle diffusion data for the adsorption of dyes onto ABent/A

C (mg/L)	Methylene blue						Crystal violet					
	Step 1			Step 2			Step 1			Step 2		
	$K_1$	$R^2$	RMSE	$K_2$	$R^2$	RMSE	$K_1$	$R^2$	RMSE	$K_2$	$R^2$	RMSE
25	1.011	0.987	0.61	0.058	0.314	0.72	0.918	0.965	0.80	0.149	0.715	0.91
50	2.161	0.950	2.76	0.090	0.668	0.56	1.614	0.995	0.48	0.352	0.803	1.81
100	3.184	0.992	1.33	0.400	0.412	4.32	2.909	0.983	1.65	0.656	0.574	4.88
200	10.492	0.987	5.81	0.386	0.479	3.34	5.056	0.989	2.23	2.247	0.890	8.24
300	13.635	0.983	8.81	0.566	0.393	5.96	6.950	0.998	1.01	2.674	0.875	10.5

range 8–11. Dyes minimal elimination percent adsorbed was got to be at pH 2 for MB and pH 3 for CV, it was 54.01% and 83.83% for MB and CV, respectively. To identify the relation between pH and MB and CV dyes adsorption, the zero charge point ( $pH_{PZC}$ ) of activated bentonite composites beads (ABent/A) should be investigated. The value of the zero charge point ( $pH_{pzc}$ ) of ABent/A was 7.04. So surface charge of activated bentonite composite is positive ( $pH < pH_{PZC}$ ). In acidic milieu, the excess of  $H^+$  resulting from the acidic medium, and the positive charge of dyes, led to a competition for the surface active sites owing to a reduction of adsorption removal. In the basic medium, the high removal of dyes on adsorbent is owing to the high interactions between the positive charge of dyes and the excess of  $OH^-$  ions. Many researchers have found the same results (Tahir and Rauf 2006; Tsai et al. 2007; Bennani Karim et al. 2009; Auta and Hameed 2012, 2013; Pawar et al. 2015).

### Temperature effect and thermodynamic data

To show temperature impact on MB and CV elimination onto ABent/A, experiments were made fixed temperatures from 283 to 313 K. The increase in the temperature is led to a fact diffusion of adsorbate molecules toward adsorbent pores, due to the reduction in solution viscosity. Moreover, the change in the temperature changes the capacity of the adsorption (Dogan et al. 2006; Karaoglu et al. 2010).

For both dyes, the removal rises up when temperature increase from 283 to 313 K, dyes adsorption is suitable at high temperatures which indicate that dyes adsorption on ABent/A beads are exothermic.

Thermodynamics data such as Gibbs free energy, enthalpy variation, and entropy variation were also given using Eqs. (14) and (15) below (Krug et al. 1976).

$$\Delta G = -RT \ln K \tag{14}$$

$$\text{Log} \left( \frac{1000 * q_e}{C_e} \right) = \frac{\Delta S^\circ}{2.303RT} - \frac{\Delta H^\circ}{2.303RT} \quad (15)$$

where  $q_e$ ,  $C_e$ ,  $R$ , and  $T$  are dyes adsorption quantity (mg/g); equilibrium concentration (mg/L); gas constant (J/mol K) and temperature (K), respectively.

Figure 8 shows the plot  $(q_e/C_e) = f(1/T)$  for the adsorption of dyes onto ABent/A; thermodynamic parameters are presented in Table 3. Gibbs' free energy negative value is an indication that dyes adsorption process is spontaneous. Enthalpy change ( $\Delta H^\circ$ ) was found to be  $-38.65 * 10^3$  and  $-61.38 * 10^2$  kJ/mol for MB and CV, respectively, which mean that adsorption, is exothermic for both dyes. The entropy change ( $\Delta S^\circ$ ) was  $-50.72$  J/mol K in case of MB and  $52.71$  J/mol K in case of CV (Kyzas et al. 2012).

### Adsorption mechanism

As the two previous Lagergren and Ho and McKay's models doesn't gives better understood for the adsorption mechanism, Weber and Morris suggest another model "intraparticle diffusion" which could provides more understanding for the mechanism of MB and CV adsorption on ABent/A. Equation 16 present the mathematic relationship of intraparticle diffusion model (Weber and Morris 1962)

$$q_t = K_i * t^{0.5} + C \quad (16)$$

where  $k_i$  is the speed constant of intraparticle diffusion model (mg/g min<sup>0.5</sup>).

Figure 9 and Table 4 show the intraparticle diffusion model and its parameters. Figure 9 shows two different sharp periods, the first one represents the diffusion of MB and CV molecule toward pores of the adsorbent. The second one characterizes the slow adsorption stage caused by the saturation of the adsorbent (Li et al. 2013).

The examination of the Fig. 9 shows us the nonlinearity of the plots for all concentrations studied which proof that the intraparticle diffusion is not the mechanism determining of the adsorption of the BM and CV on ABent/A beads, it exists, but it is done at the same time as the other mechanisms of diffusion. Table 5 shows the comparison between the prepared adsorbents in this study with others various adsorbents used by other researchers.

### Reusability study of ABent/A

The results of the regeneration of MB and CV dyes from ABent/A are shown in Fig. 10.

MB regeneration was evaluated using HCl solutions (0.01 and 0.1 M). Both 0.1 and 0.01 M hydrochloric acid solutions were effective in MB regeneration, and they show 98.92% and 97.04% of MB regeneration in the first cycle. With the increase in cycle numbers, the MB desorption percentage decreases slightly for both 0.1 and 0.01 M hydrochloric acid solution until it reaches 91.22% and 89.47% after six cycles.

CV desorption was studied using 0.5 M acetic acid solution, 0.5 M potassium chloride solution, 100% ethanol and 0.5 M potassium chloride prepared in the mixture ethanol/water (0.5%/0.5%). As shown in Fig. 10, the CV regeneration percentages were 30%, 25%, 12% using 0.5 M acetic acid solution, 0.5 M KCl solution and 100% ethanol solution, respectively. When the 0.5 M KCl in ethanol/water (50/50, V/V) was utilized, adsorption/desorption cycle was come up to 95%. Same findings reported by Eren et al. (2010).

### Conclusion

This work investigates the valorization of natural Algerian bentonite by using it in the preparation of very efficient adsorbent ABent/A, Adsorption study was carried in batch system according to several changing operational conditions. The results of MB and CV adsorption showed that all studied parameters effect adsorption process. Lagergren and Ho and McKay's models were very suitable for the description of MB and CV adsorption processes, respectively.

MB and CV isotherms were well-described using Langmuir isotherm model justifying a monolayer and homogeneous adsorption. MB and CV adsorption process onto ABent/A was exothermic. Regeneration study showed that dyes were successfully desorbed using 0.01 M hydrochloric acid and 0.5 M potassium chloride prepared in the mixture ethanol/water (0.5%/0.5%), for MB and CV, respectively. Activated bentonite/alginate composites are low-cost, effective and regenerable adsorbent, which give a promising prospect for contaminated wastewaters treatment.

**Table 5** Comparison of dyes adsorption amounts onto various adsorbents

Adsorbents	Dyes	Kinetic and isotherm models	Maximum adsorption capacity (mg/g)	References
Acid-activated bentonite	MB	Pseudo-second-order Langmuir	151.43	This study
Activated bentonite/alginate composite beads		Pseudo-second-order Langmuir	780.59	This study
Magnetic nanoparticles CS-MCM		Pseudo-second-order Langmuir	31.80	Yan et al. (2013)
Magnetic nanoparticles CS-Glu-MCM		Pseudo-second-order Langmuir	185.1	Yan et al. (2013)
Alginate–bentonite–activated carbon composite beads		Pseudo-second-order Freundlich	994.06	Benhouria et al. (2015)
Coffee ground-sodium-alginate beads		Pore diffusion model Sips	622.70	Jung et al. (2016)
Activated-organo-bentonite beads		Pseudo-second-order Langmuir	769	Belhouchat et al. (2017)
Acid-activated bentonite	CV	Pseudo-second-order Langmuir	278.80	This study
Activated bentonite/alginate composite beads		Pseudo-second-order Langmuir	546.53	This study
Magnetic nanoparticles CS-MCM		Pseudo-second-order Langmuir	82.20	Yan et al. (2013)
Magnetic nanoparticles CS-Glu-MCM		Pseudo-second-order Langmuir	390	Yan et al. (2013)
Hebei province bentonite HB-Bt		–	800	Wei et al. (2009)
Inner Mongoli autonomous bentonite NM-Bt		–	500	Wei et al. (2009)
magnetic carbon–iron oxide nanocomposite		–	810.70	Singh et al. (2011)
Acid-activated bentonite		Pseudo-nth order Redlich–Peterson Langmuir	582.40	Oladipo and Gazi (2014)

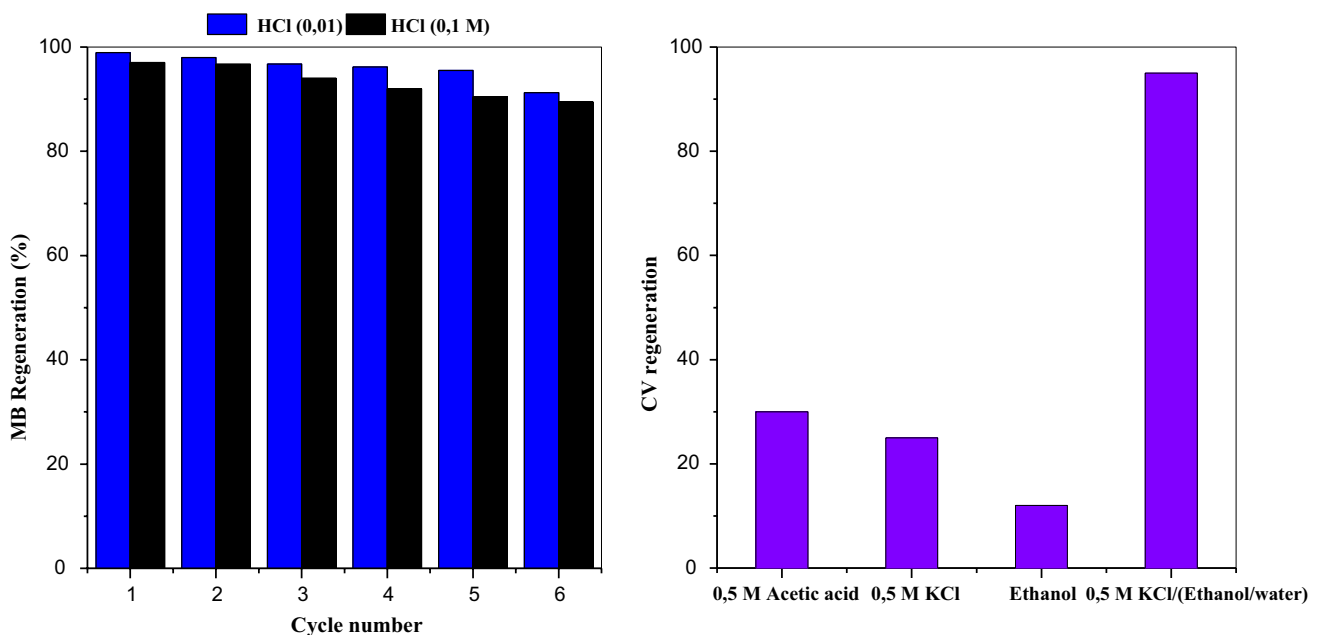


**Fig. 10** Methylene blue and crystal violet regeneration

**Open Access** This article is licensed under a Creative Commons Attribution 4.0 International License, which permits use, sharing, adaptation, distribution and reproduction in any medium or format, as long as you give appropriate credit to the original author(s) and the source, provide a link to the Creative Commons licence, and indicate if changes were made. The images or other third party material in this article are included in the article's Creative Commons licence, unless indicated otherwise in a credit line to the material. If material is not included in the article's Creative Commons licence and your intended use is not permitted by statutory regulation or exceeds the permitted use, you will need to obtain permission directly from the copyright holder. To view a copy of this licence, visit <http://creativecommons.org/licenses/by/4.0/>.

## References

- Abbasi AR, Karimi M, Daasbjerg K (2017) Efficient removal of crystal violet and methylene blue from wastewater by ultrasound nanoparticles Cu-MOF in comparison with mechanosynthesis method. *Sonochem, Ultrason*. <https://doi.org/10.1016/j.ultsonch.2017.01.007>
- Abdollahi M, Alboofetileh M, Rezaei M, Behrooz R (2013) Comparing physico-mechanical and thermal properties of alginate nanocomposite films reinforced with organic and/or inorganic nanofillers. *Food Hydrocoll* 32:416–424
- AbouTaleb MF, Hegazy DE, Ismail SA (2012) Radiation synthesis, characterization and dye adsorption of alginate–organophilic montmorillonite nanocomposite. *Carbohydr Polym* 87:2263–2269
- Anirudhan TS, Ramachandran M (2015) Adsorptive removal of basic dyes from aqueous solutions by surfactant modified bentonite clay (organoclay): kinetic and competitive adsorption isotherm. *Process Saf Environ Prot* 95:215–225
- Auta M, Hameed BH (2012) Modified mesoporous clay adsorbent for adsorption isotherm and kinetics of methylene blue. *Chem Eng J* 198–199:219–227
- Auta M, Hameed BH (2013) Acid modified local clay beads as effective low-cost adsorbent for dynamic adsorption of methylene blue. *J Ind Eng Chem* 19:1153–1161
- Auta M, Hameed BH (2014) Chitosan–clay composite as highly effective and low-cost adsorbent for batch and fixed-bed adsorption of methylene blue. *Chem Eng J* 237:352–361
- Belhouchat N, Zaghoulane-Boudiaf H, Viseras C (2017) Removal of anionic and cationic dyes from aqueous solution with activated organo-bentonite/sodium alginate encapsulated beads. *Appl Clay Sci* 135:9–15
- Benhouria A, Islam MdA, Zaghoulane-Boudiaf H, Boutahala M, Hameed BH (2015) Calcium alginate–bentonite–activated carbon composite beads as highly effective adsorbent for methylene blue. *Chem Eng J* 270:621–630
- Bennani Karim A, Mounir B, Hachkar M, Bakasse M, Yaacoubi A (2009) Removal of Basic Red 46 dye from aqueous solution by adsorption onto Moroccan clay. *J Hazard Mater* 168:304–309
- Bertolini TCR, Izidoro JC, Magdalena CP, Fungaro DA (2013) Adsorption of crystal violet dye from aqueous solution onto zeolites from coal fly and bottom ashes. *Electron J Chem* 5(3):179–191
- Boualla N, Benziane A (2011) Étude expérimentale sur l'élimination des nitrates par adsorption sur des argiles activées et non activées de la sebkha d'Oran. *Afr Sci* 07(2):56–73
- Chen YG, He Y, Ye WM, Jia LY (2015) Competitive adsorption characteristics of Na(I)/Cr(III) and Cu(II)/Cr(III) on GMZ bentonite in their binary solution. *J Ind Eng Chem* 26:335–339
- Cheng Y, Lu L, Zhang W, Shi J, Cao Y (2012) Reinforced low density alginate-based aerogels: preparation, hydrophobic modification and characterization. *Carbohydr Polym* 88:1093–1099
- Dellamatrice PM, Silva-Stenico ME, Beraldo de Moraes LA, Fiore MF, Monteiro RTR (2017) Degradation of textile dyes by cyanobacteria. *Braz J Microbiol* 48:25–31
- Derafa G, Zaghoulane-Boudiaf H, Ibbora CV (2018) Preparation and characterization of new low cost adsorbent beads based on activated bentonite encapsulated with calcium alginate for removal of 2, 4-dichlorophenol from aqueous medium. *Int J Biol Macromol* 115:257–265
- Dogan M, Alkan M, Demirbas O, Ozdemir Y, Ozmetin C (2006) Adsorption kinetics of maxilon blue GRL onto sepiolite from aqueous solutions. *Chem Eng J* 124:89–101
- Dubinin MM, Radushkevich LW (1947) Equation of the characteristic curve of activated charcoal. *Proc Acad Sci Phys Chem Sect* 55:331–333
- Elmoubarki R, Mahjoubi FZ, Tounsadi H, Moustadraf J, Abdennouri M, Zouhri A, ElAlbani A, Barka N (2017) Adsorption of textile dyes on raw and decanted Moroccan clays: kinetics, equilibrium and thermodynamics. *Water Resour Ind*. <https://doi.org/10.1016/j.wri.2014.11.001>
- Ely A, Baudau M, Kankou MOSAO, Basly J-P (2011) Copper and nitrophenol removal by low cost alginate/Mauritanian clay composite beads. *Chem Eng J* 178:168–174
- Eren E, Cubuk O, Ciftci H, Eren B, Caglar B (2010) Adsorption of basic dye from aqueous solutions by modified sepiolite: equilibrium, kinetics and thermodynamics study. *Desalination* 252:88–96
- Freundlich HMF (1906) Over the adsorption in solution. *J Phys Chem* 57:385–471
- Fu J, Chen Z, Wang M, Liu S, Zhang J, Zhang J, Han R, Xu Q (2015) Adsorption of methylene blue by a high-efficiency adsorbent (polydopamine microspheres): kinetics, isotherm, thermodynamics and mechanism analysis. *Chem Eng J* 259:53–61
- Guz L, Curutchet G, Torres Sanchez RM, Candal R (2014) Adsorption of crystal violet on montmorillonite (or iron modified 3 montmorillonite) followed by degradation through Fenton or 4 photo-Fenton type reactions. *Environ Chem Eng J*. <https://doi.org/10.1016/j.jece.2014.02.007>
- Hassani A, Soltani RDC, Karaca S, Khataee A (2015) Preparation of montmorillonite–alginate nanobiocomposite for adsorption of a textile dye in aqueous phase: isotherm, kinetic and experimental design approaches. *J Ind Eng Chem* 21:1197–1207
- Ho YS, McKay G (1999) Pseudo-second order model for sorption processes. *Process Biochem* 34:451–465
- Huang Z, Li Y, Chen W, Shi J, Zhang N, Wang X, Li Z, Gao L, Zhang Y (2017) Modified bentonite adsorption of organic pollutants of dye wastewater. *Mater Chem Phys*. <https://doi.org/10.1016/j.matchemphys.2017.09.028>
- Jauris IM, Fagan SB, Adebayo MA, Machado FM (2016) Adsorption of acridine orange and methylene blue synthetic dyes and anthracene on single wall carbon nanotubes: a first principle approach. *Comput Theor Chem* 1076:42–50
- Jung KW, Choi BH, Hwang MJ, Jeong TU, Ahn KH (2016) Fabrication of granular activated carbons derived from spent coffee grounds by entrapment in calcium alginate beads for adsorption of acid orange 7 and methylene blue. *Bioresour Technol* 219:185–195
- Karaoglu MH, Dogan M, Alkan M (2010) Kinetic analysis of reactive blue 221 adsorption on kaolinite. *Desalination* 256:154–165
- Krug R, Hunter W, Grieger R (1976) Enthalpy–entropy compensation. 1. Some fundamental statistical problems associated with the analysis of van't Hoff and Arrhenius data. *J Phys Chem* 80:2335–2341
- Kumar M, Tamilarasan R, Sivakumar V (2013) Adsorption of Victoria blue by carbon/Ba/alginate beads: kinetics, thermodynamics and isotherm studies. *Carbohydr Polym* 98:505–513
- Kuppasamy S, Venkateswarlu K, Thavamani P, Lee YB, Naidu R, Megharaj M (2017) Quercus robur acorn peel as a novel coagulating adsorbent for cationic dye removal from aquatic ecosystems. *Ecol Eng* 101:3–8

- Kyzas GZ, Lazaridis NK, Mitropoulos ACH (2012) Removal of dyes from aqueous solution with untreated coffee residues as potential low-cost adsorbents: equilibrium, reuse and thermodynamic approach. *Chem Eng J* 189:148–159
- Lagergren S (1898) Zur theorie der sogenannten Adsorption gelöster stoffe, *Kungliga Svenska Vetenskapsakademiens. Handlingar* 24(4):1–39
- Langmuir I (1918) The constitution and fundamental properties of solids and liquids. *J Am Chem Soc* 40:1361–1403
- Lezehari M, Basly JPH, Baudu M, Bouras O (2010) Alginate encapsulated pillared clays: removal of a neutral/anionic biocide (pentachlorophenol) and a cationic dye (safranin) from aqueous solutions. *Colloid Surf A* 366:88–94
- Li Y, Du Q, Liu T, Peng X, Wang J, Sun J, Wang Y, Wu S, Wang Z, Xia Y, Xia L (2013) Comparative study of methylene blue dye adsorption onto activated carbon, graphene oxide, and carbon nanotubes. *Chem Eng Res Des* 91:361–368
- Li S, Wang X, He Q, Chen Q, Xu Y, Yang H, Lü M, Wei F, Liu X (2016) Synergistic effects in N-K<sub>2</sub>Ti<sub>4</sub>O<sub>9</sub>/UiO-66-NH<sub>2</sub> composites and their photocatalysis degradation of cationic dyes. *Chin J Catal* 37:367–377
- Mittal A, Mittal J, Malviya A, Kaur D, Gupta VK (2010) Adsorption of hazardous dye crystal violet from wastewater by waste materials. *J Colloid Interface Sci* 343:463–473
- Nandi BK, Goswami A, Purkait MK (2009) Adsorption characteristics of brilliant green dye on kaolin. *J Hazard Mater* 161:387–395
- Oladipo AA, Gazi M (2014) Enhanced removal of crystal violet by low cost alginate/acid activated bentonite composite beads: optimization and modelling using non-linear regression technique. *J Water Proc Eng.* <https://doi.org/10.1016/j.jwpe.2014.04.007>
- Pandi K, Viswanathan N (2014) Synthesis of alginate bioencapsulated nano-hydroxyapatite composite for selective fluoride sorption. *Carbohydr Polym* 112:662–667
- Papic S, Koprivanac N, Loncaric Bozic A (2000) Removal of reactive dyes from wastewater using Fe(III) coagulant. *JSDC* 116:352–358
- Papic S, Koprivanac N, Bozic AL, Metes A (2004) Removal of some reactive dyes from synthetic wastewater by combined Al(III) coagulation/carbon adsorption process. *Dyes Pigment* 62:291–298
- Pawar RR, Lalhmunsiam, Bajaj HC, Lee SM (2015) Activated bentonite as a low cost adsorbent for the removal of Cu(II) and Pd(II) from aqueous solutions: batch and column studies. *J Ind Eng Chem.* <https://doi.org/10.1016/j.jiec.2015.11.014>
- Peng Y, Wang KK, Liu T, Xu J, Xu BJ (2016) Synthesis of one-dimensional Bi<sub>2</sub>O<sub>3</sub>-Bi<sub>2</sub>O<sub>2.33</sub> heterojunctions with high interface quality for enhanced visible light photocatalysis in degradation of high-concentration phenol and MO dyes. *Appl Catal B Environ.* <https://doi.org/10.1016/j.apcatb.2016.11.011>
- Rafatullah M, Sulaiman O, Hashima R, Ahmad A (2010) Adsorption of methylene blue on low-cost adsorbents: a review. *J Hazard Mater* 177:70–80
- Rager T, Geoffroy A, Hilfiker R, Storey GMD (2012) The crystalline state of methylene blue: a zoo of hydrates. *Phys Chem Chem Phys* 14:8074–8082
- Sandoval A, Hernández-Ventura C, Klimova TE (2016) Titanate nanotubes for removal of methylene blue dye by combined adsorption and photocatalysis. *Fuel.* <https://doi.org/10.1016/j.fuel.2016.11.007>
- Singh KP, Gupta S, Singh AK, Sinha S (2011) Optimizing adsorption of crystal violet dye from water by magnetic nanocomposite using response surface modeling approach. *J Hazard Mater* 186:1462–1473
- Tahir SS, Rauf N (2006) Removal of a cationic dye from aqueous solutions by adsorption onto bentonite clay. *Chemosphere* 63:1842–1848
- Tan WS, Ting ASY (2014) Alginate-immobilized bentonite clay: adsorption efficacy and reusability for Cu(II) removal from aqueous solution. *Bioresour Technol* 160:115–118
- Tezcan F, Günister E, Özen G, Erim FB (2012) Biocomposite films based on alginate and organically modified clay. *Int J Biol Macromol* 50:1165–1168
- Toth J (1962) *Acta Chimica Academiae Scientiarum Hungaricae*, vol 32. Akademiai Kiado, Budapest, pp 39–45
- Tsai WT, Hsu HC, Su TY, Lin KY, Lin CM, Dai TH (2007) The adsorption of cationic dye from aqueous solution onto acid-activated andesite. *J Hazard Mater* 147:1056–1062
- Vijaya Y, Popuri SR, Boddu VM, Krishnaiah A (2008) Modified chitosan and calcium alginate biopolymer sorbents for removal of nickel(II) through adsorption. *Carbohydr Polym* 72:261–271
- Wang Y, Wang W, Wang A (2013) Efficient adsorption of methylene blue on an alginate-based nanocomposite hydrogel enhanced by organo-illite/smectite clay. *Chem Eng J* 228:132–139
- Weber WJ, Morris JC (1962) Water pollution symposium. In: *Proceedings of the second international conference*. Pergamon, Oxford, pp 231–266
- Wei J, Zhu R, Zhu J, Ge F, Yuan P, He H, Ming C (2009) Simultaneous sorption of crystal violet and 2-naphthol to bentonite with different CECs. *J Hazard Mater* 166:195–199
- Yan H, Li H, Yang H, Li A, Cheng R (2013) Removal of various cationic dyes from aqueous solutions using a kind of fully biodegradable magnetic composite microspheres. *Chem Eng J* 223:402–411
- Zaghouane-Boudiaf H, Boutahala M (2011) Kinetic analysis of 2,4,5-trichlorophenol adsorption onto acid-activated montmorillonite from aqueous solution. *Int J Miner Process* 100:72–78
- Zaghouane-Boudiaf H, Boutahala M, Sahnoun S, Tiar C, Gomri F (2014) Adsorption characteristics, isotherm, kinetics, and diffusion of modified natural bentonite for removing the 2, 4, 5-trichlorophenol. *Appl Clay Sci* 90:81–87

**Publisher's Note** Springer Nature remains neutral with regard to jurisdictional claims in published maps and institutional affiliations.